Supporting Information for

Thermo-responsive fluorescence of AIE-active poly(*N*-isopropylacrylamides) labeled with highly twisted bis(*N*,*N*-dialkylamino)arenes

Shunsuke Sasaki[a] and Gen-ichi Konishi[a,*]

[a]*Department of Chemical Science and Engineering, Tokyo Institute of Technology, O-okayama, Meguro-ku, Tokyo, 152-8552, Japan. E-mail: konishi.g.aa@m.titech.ac.jp; Fax: +81-3-5734-2888; Tel: +81-3-5734-2321*

S1. Instruments and methods

(1) General procedures

All the reagents and solvents (spectroscopic grade) were obtained from commercial sources and used without further purification. All ^{1}H NMR and ^{13}C NMR spectra were recorded on a 500 MHz BRUKER avance III or 300 MHz BRUKER DPX300 spectrometer with tetramethylsilane (TMS) as the internal standard. FT-IR spectra were recorded on a JASCO FT-IR 469 plus spectrometer. Melting points were recorded on a Yanaco micro melting point MP-500P apparatus. MS spectra (FAB+) were obtained on a JEOL JMS700 mass spectrometer. Size-exclusion chromatography (SEC) was performed at 30 °C using a JASCO PU-1580 / UV-1570 / RI-1530 system equipped with a set of Tosoh TSK-gel G5000H$_{XL}$ and TSK-gel G4000H$_{XL}$ columns. The eluent for SEC was DMF containing 0.01 M LiBr (0.70 mL min^{-1}). The number-average molecular weight (M_n), weight-average molecular weight (M_w), and the polydispersity index (M_w/M_n) of the polymers were calculated on the basis of polystyrene calibrations.

All photophysical measurements of low-molecular-weight compounds performed in solutions were carried out using dilute solutions (solute concentration: 1.0 x 10^{-5} M) in quartz cells (path length: 1 cm) at room temperature (293 K). Unless otherwise noted, all sample solutions were deaerated by sparging with argon gas for 15 min prior to the measurements. UV-Vis spectra were recorded on a JASCO V-670 UV-Vis spectrophotometer. Fluorescence spectra were recorded on a JASCO FP-6500

spectrofluorometer. Absolute quantum yields were measured on a Hamamatsu Photonics Quantaurus QY. Fluorescence lifetimes were measured at the most intense peaks using a Hamamatsu Photonics OB 920 Fluorescence Lifetime spectrometer equipped with LEDs lamp (343 nm). Experimental procedures specific to the photophysical measurements of PNIPAM and its gels are described in the experimental section of the manuscript.

S2. Materials

Unless otherwise noted, all reagents and chemicals were used as received without further purification. Potassium *tert*-butoxide, 9,10-dibromoanthracene, 1-bromoethane, 1-methyl-2-pyrrolidine, 3-(*N*-methylamino)-1-propanol, *N*-methyl-3-chloropropylamine hydrochloride, triethylamine, methacryloyl chloride, bromine, 5-amino-1-pentanol, *tert*-butyldiphenylchlorosilane, a 1 M THF solution of tetrabutylammmonium fluoride, and *N*-isopropyl acrylamide were obtained from TCI (Tokyo, Japan). Cesium carbonate, sodium hydroxide, imidazole, and 2,2'-azobisisobutyronitrile were purchased from Wako Pure Chem (Tokyo, Japan). Dehydrated 1,4-dioxane, sodium bromide, potassium iodide, and dehydrated tetrahydrofuran were obtained from Kanto Chem (Tokyo, Japan). Magnesium sulphate, potassium carbonate, methyl iodide, spectrograde *n*-hexane, THF, acetonitrile, and methanol were purchased from Nacalai Tasque (Kyoto, Japan). PEPPSI^{TM}-IPr catalyst and 2,3-dimethylnaphthalene were purchased from Sigma-Aldrich Japan (Tokyo, Japan). The pure water employed in the photophysical measurements was prepared using a Milli-Q® water purification system (Merck Millipore, United States).

S3. NMR spectra

(1) Terminal-functionalized 9,10-bis(*N*,*N*-dialkylamino)anthracene

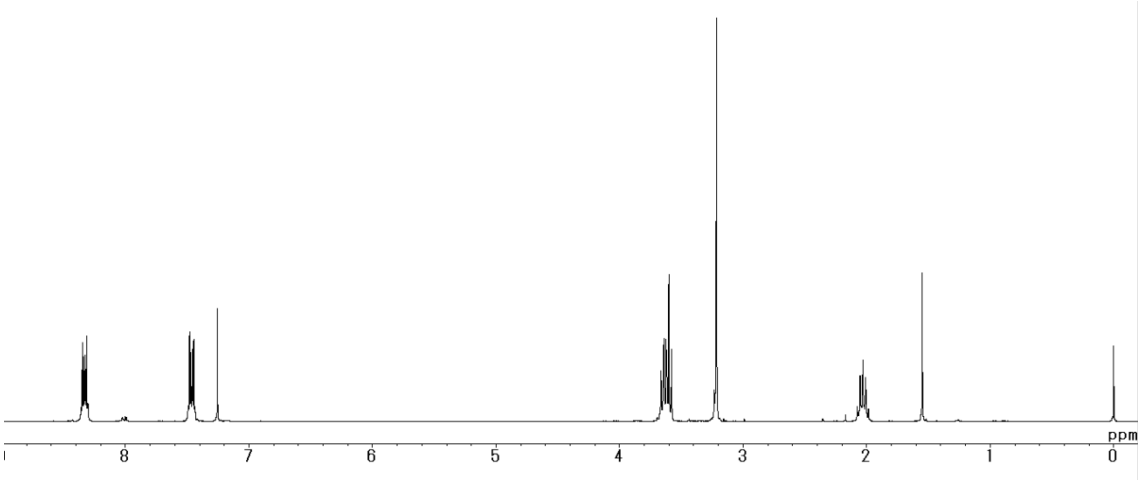

Fig. S1. ^{1}H NMR spectrum of 9,10-bis(*N*-(3-chloropropyl)-*N*-methylamino)anthracene (**3**) (300 MHz, $CDCl_3$).

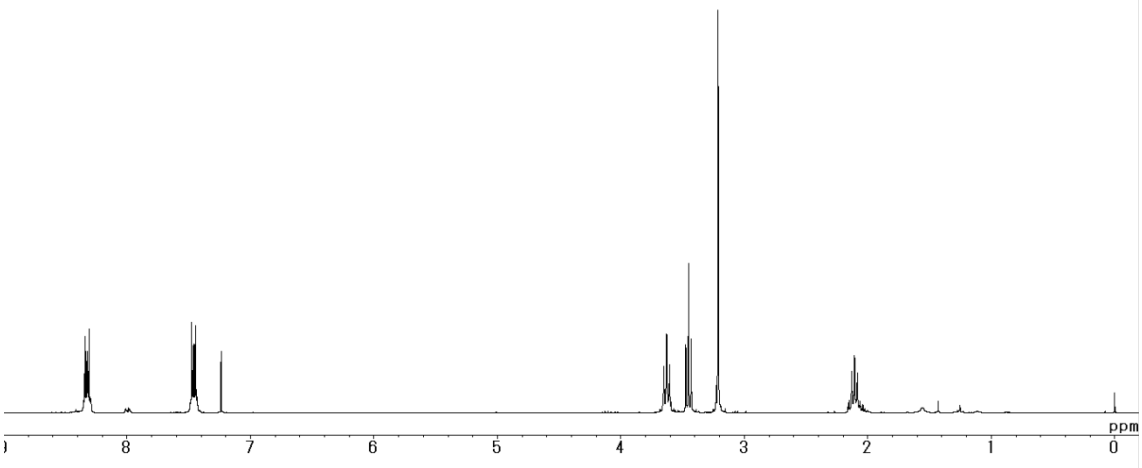

Fig. S2. ^{1}H NMR spectrum of 9,10-bis(*N*-(3-bromopropyl)-*N*-methylamino)anthracene (**4**) (300 MHz, $CDCl_3$).

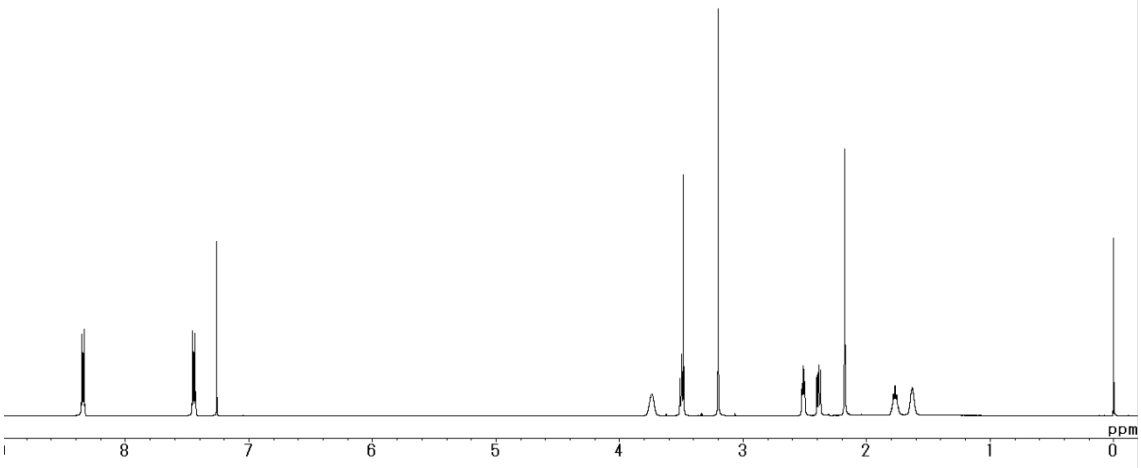

Fig. S3. ^{1}H NMR spectrum of 9,10-bis(*N*-(3'-(*N*''-(3''-hydroxyprop-1''-yl)-*N*''-methylamino))prop-1'-yl)-*N*-methylamino)anthracene (**6**) (500 MHz, $CDCl_3$).

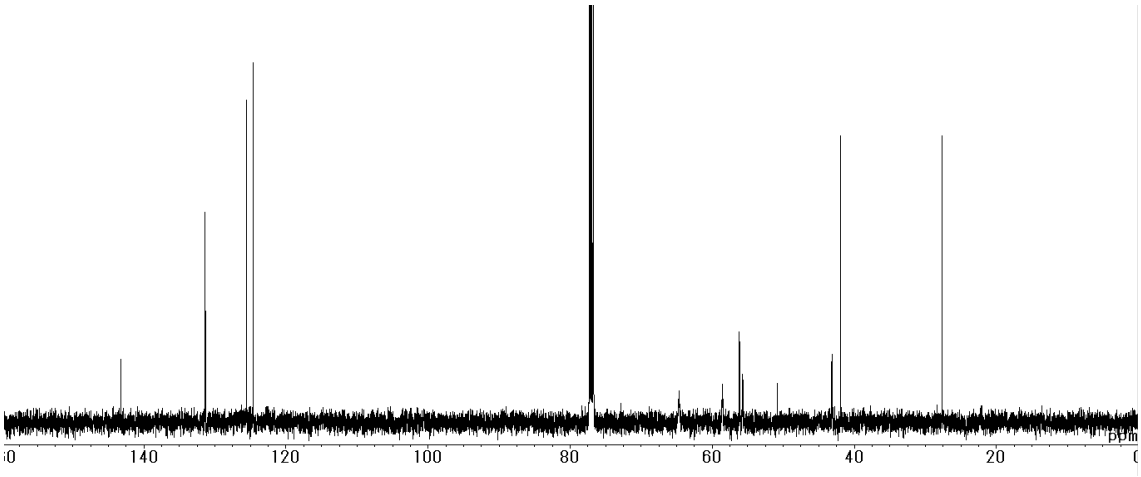

Fig. S4. ^{13}C NMR spectrum of 9,10-bis(*N*-(3'-(*N*''-(3''-hydroxyprop-1''-yl)-*N*''-methylamino))prop-1'-yl)-*N*-methylamino)anthracene (**6**) (125 MHz, $CDCl_3$).

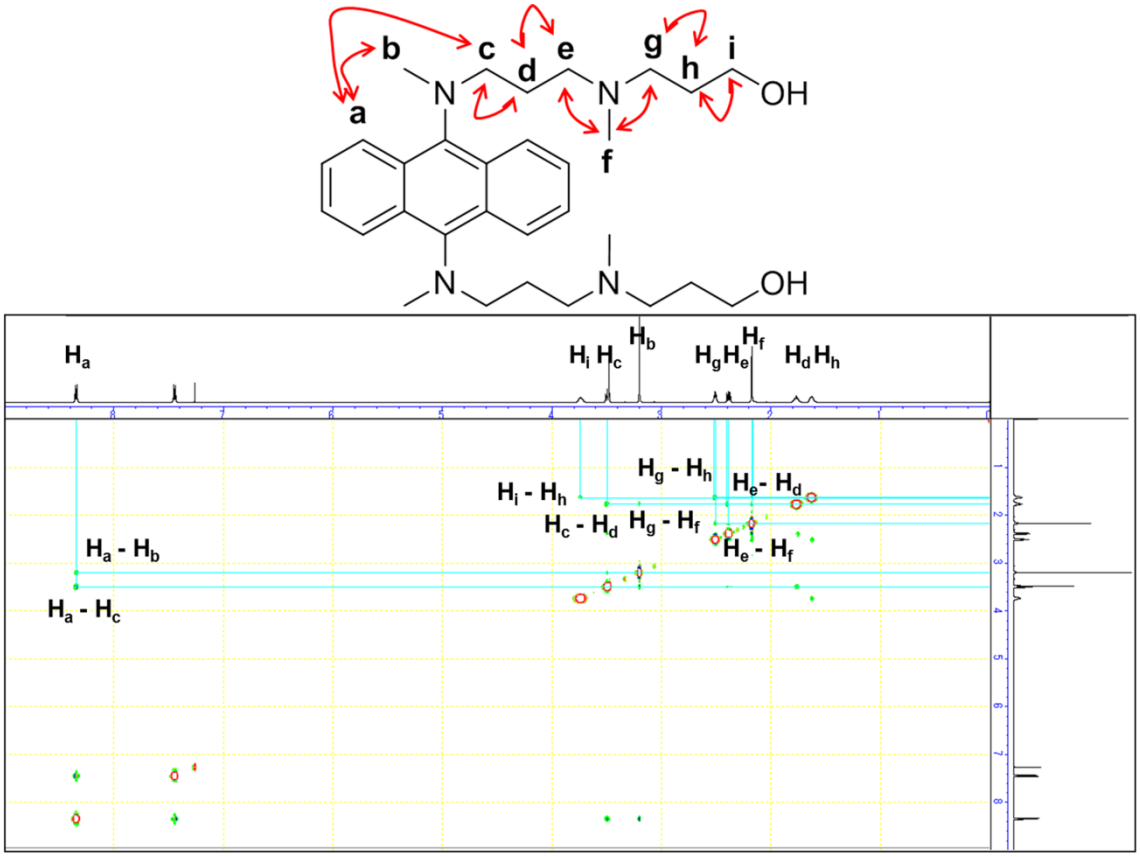

Fig. S5. NOESY spectrum of 9,10-bis(*N*-(3'-(*N*''-(3''-hydroxyprop-1''-yl)-*N*''-methylamino))prop-1'-yl)-*N*-methylamino)anthracene (**6**) (500 MHz, $CDCl_3$). Several important signals are picked up and assigned as indicated by red arrows. The proton H_f experienced detectable NOE effects from both H_e and H_g, which supports the assigned chemical structure of **6**.

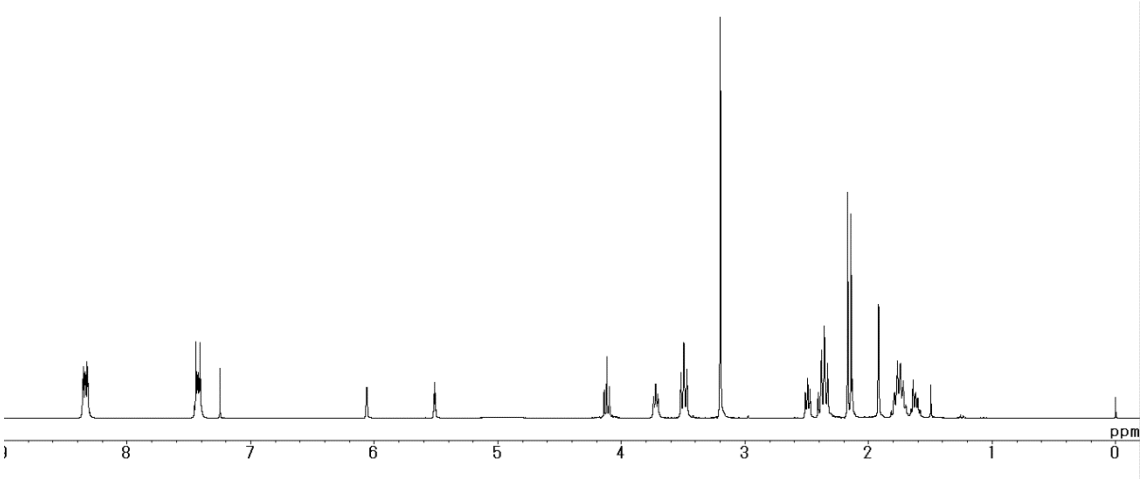

Fig. S6. ^1H NMR spectrum of methacrylate-monofunctionalized 9,10-bis(*N*,*N*-dialkylamino)anthracene (**ANTH-monomer**) (300 MHz, $CDCl_3$).

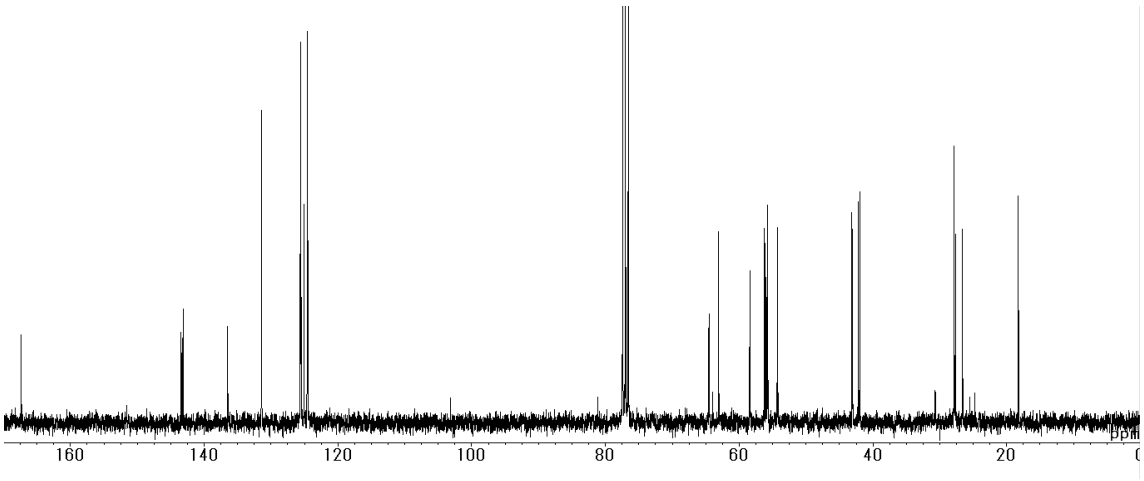

Fig. S7. ^{13}C NMR spectrum of methacrylate-monofunctionalized 9,10-bis(*N*,*N*-dialkylamino)anthracene (**ANTH-monomer**) (75 MHz, $CDCl_3$).

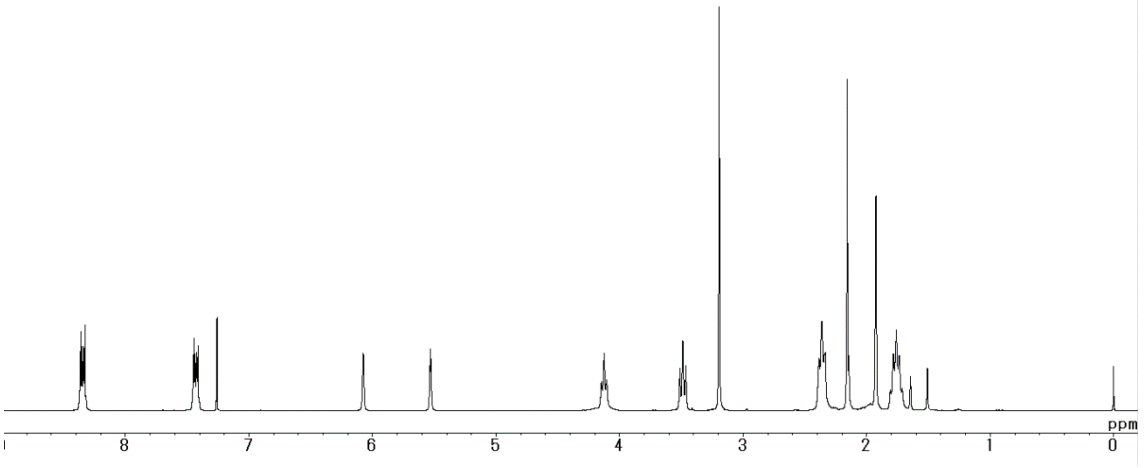

Fig. S8. ^{1}H NMR spectrum of methacrylate-difunctionalized 9,10-bis(*N*,*N*-dialkylamino)anthracene (**ANTH-linker**) (300 MHz, $CDCl_3$).

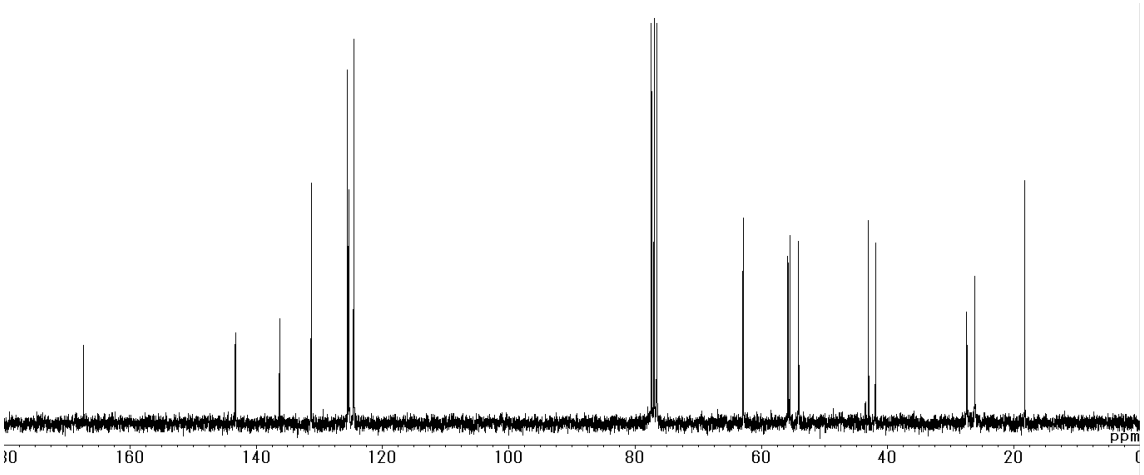

Fig. S9. ^{13}C NMR spectrum of methacrylate-difunctionalized 9,10-bis(*N*,*N*-dialkylamino)anthracene (**ANTH-linker**) (75 MHz, $CDCl_3$).

(2) Terminal-functionalized 1,4-bis(*N*,*N*-dialkylamino)-2,3-dimethylnaphthalene

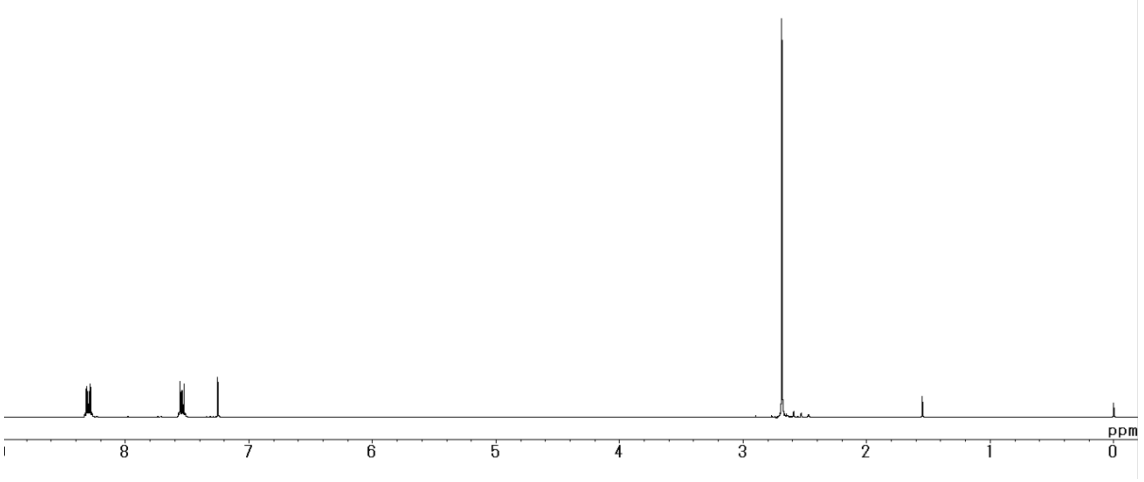

Fig. S10. ^{1}H NMR spectrum of 1,4-dibromo-2,3-dimethylnaphthalene (**9**) (300 MHz, $CDCl_3$).

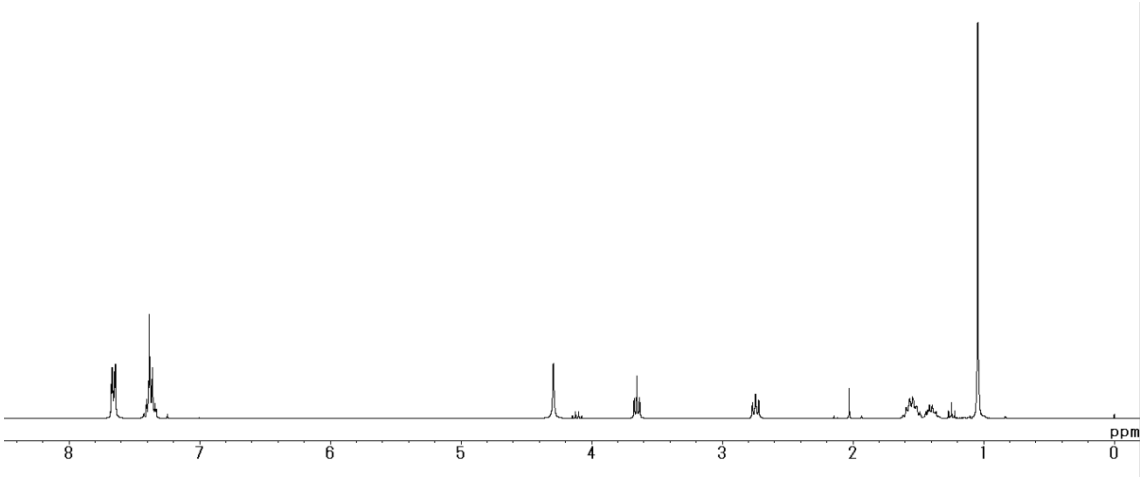

Fig. S11. ^{1}H NMR spectrum of 5-(*tert*-butyldiphenylsiloxy)pentan-1-amine (**11**) (300 MHz, $CDCl_3$).

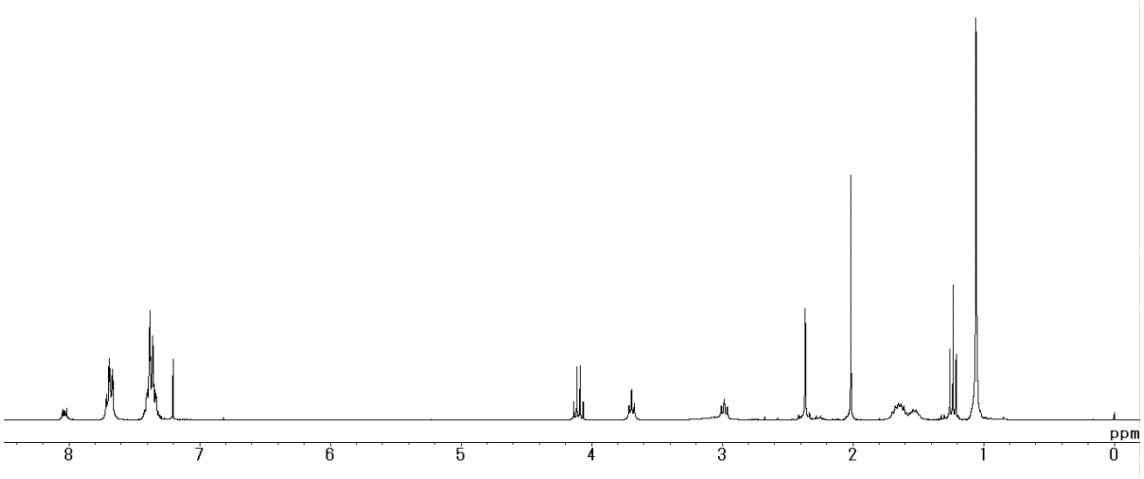

Fig. S12. ^{1}H NMR spectrum of 1,4-bis(*N*-(5-(*tert*-butyldiphenylsiloxy)-pent-1-yl)amino)-2,3-dimethylnaphthalene (**12**) (300 MHz, $CDCl_3$).

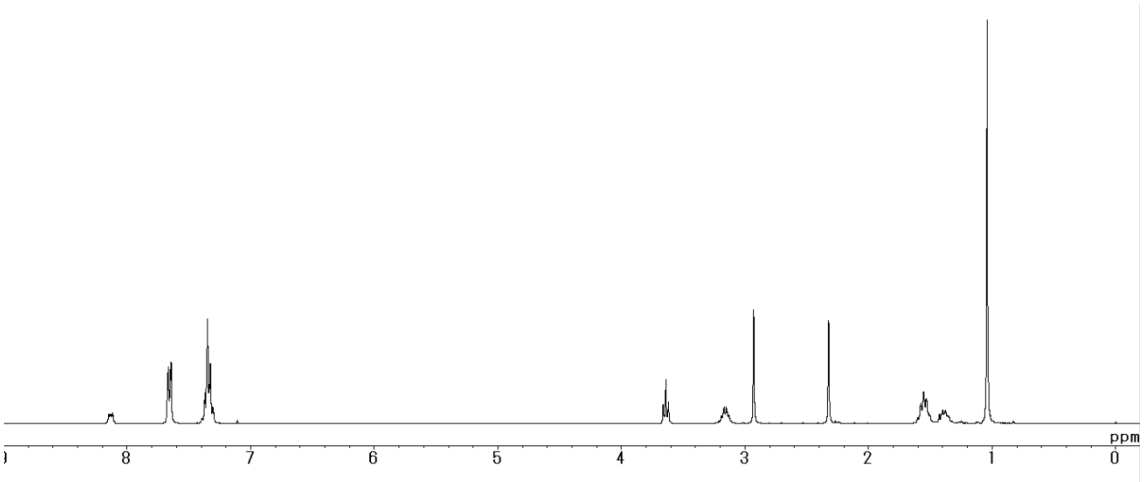

Fig. S13. ^{1}H NMR spectrum of 1,4-bis(*N*-(5-(*tert*-butyldiphenylsiloxy)-pent-1-yl)-*N*-methylamino)-2,3-dimethylnaphthalene (**13**) (300 MHz, $CDCl_3$).

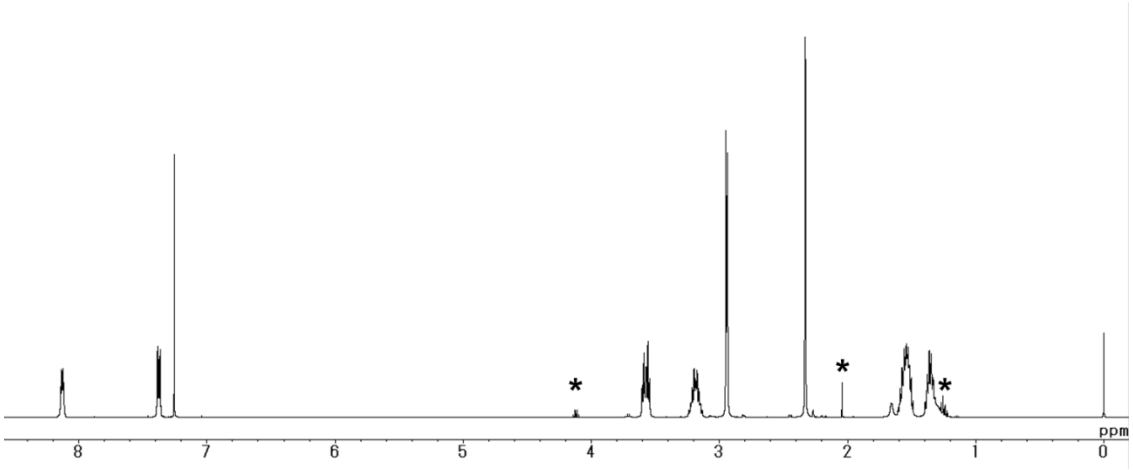

Fig. S14. ^{1}H NMR spectrum of 1,4-bis(*N*-(hydroxypent-5-yl)-*N*-methylamino)-2,3-dimethylnaphthalene (**14**) (500 MHz, $CDCl_3$). Trace amounts of ethyl acetate remained as signified by asterisk.

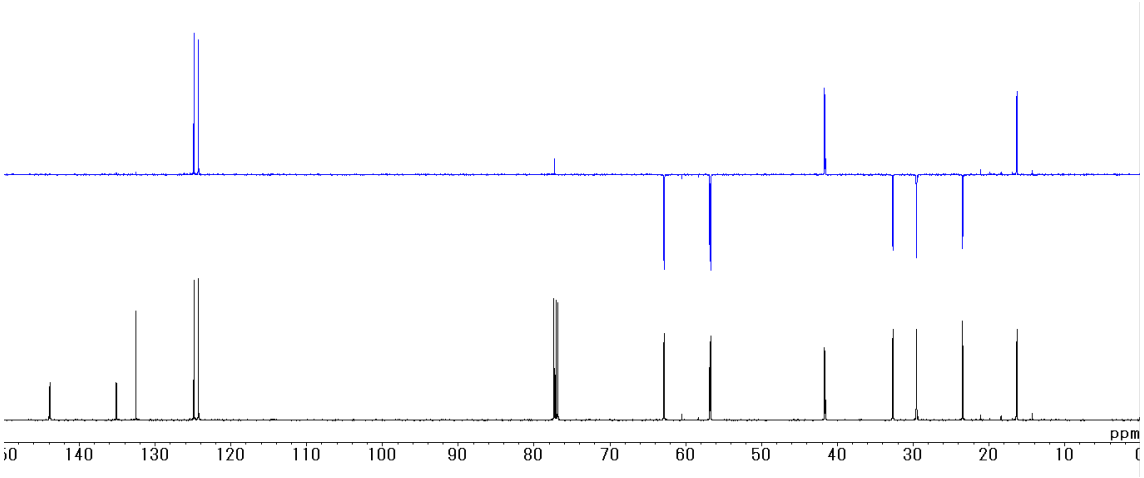

Fig. S15. (top) DEPT-135° and (bottom) ^{13}C NMR spectra of 1,4-bis(*N*-(hydroxypent-5-yl)-*N*-methylamino)-2,3-dimethylnaphthalene (**14**) (125 MHz, $CDCl_3$).

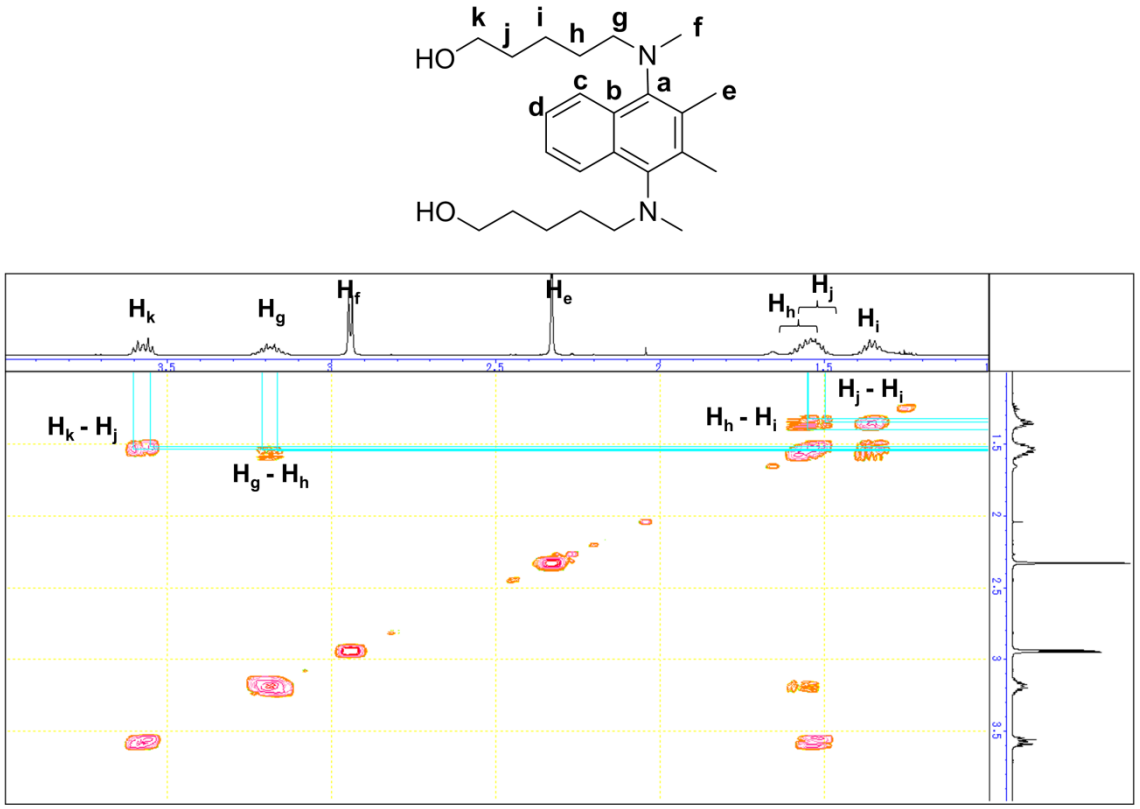

Fig. S16. ^{1}H – ^{1}H COSY spectrum (enlarged view of the aliphatic region) of 1,4-bis(*N*-(hydroxypent-5-yl)-*N*-methylamino)-2,3-dimethylnaphthalene (**14**) (500 MHz, $CDCl_3$).

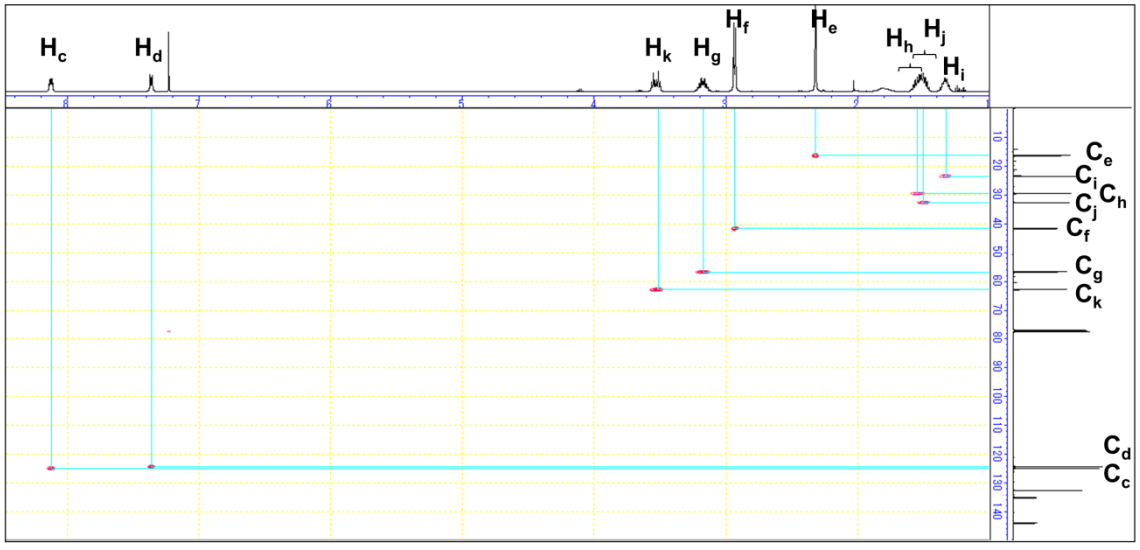

Fig. S17. ^{1}H – ^{13}C HSQC spectrum of 1,4-bis(*N*-(hydroxypent-5-yl)-*N*-methylamino)-2,3-dimethylnaphthalene (**14**) (500 MHz, $CDCl_3$).

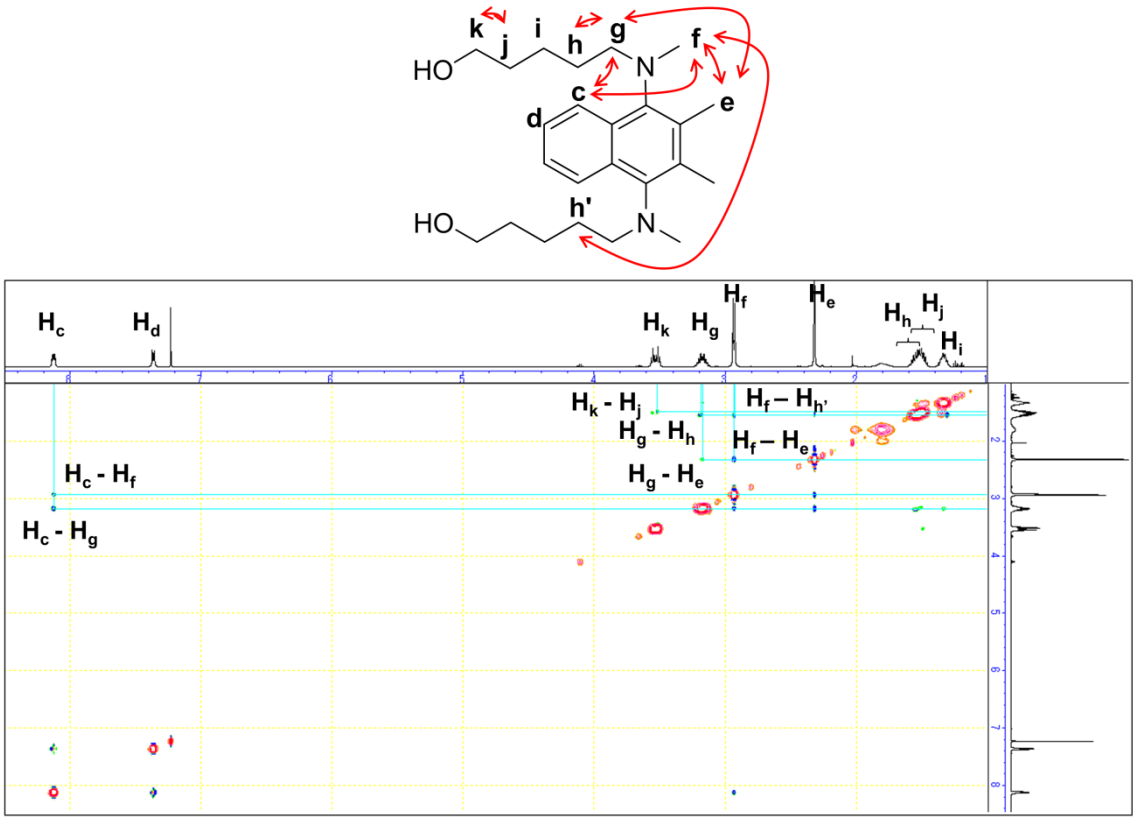

Fig. S18. NOESY spectrum of 1,4-bis(*N*-(hydroxypent-5-yl)-*N*-methylamino)-2,3-dimethylnaphthalene (**14**) (500 MHz, $CDCl_3$). Several important signals are picked up and assigned as indicated by red arrows.

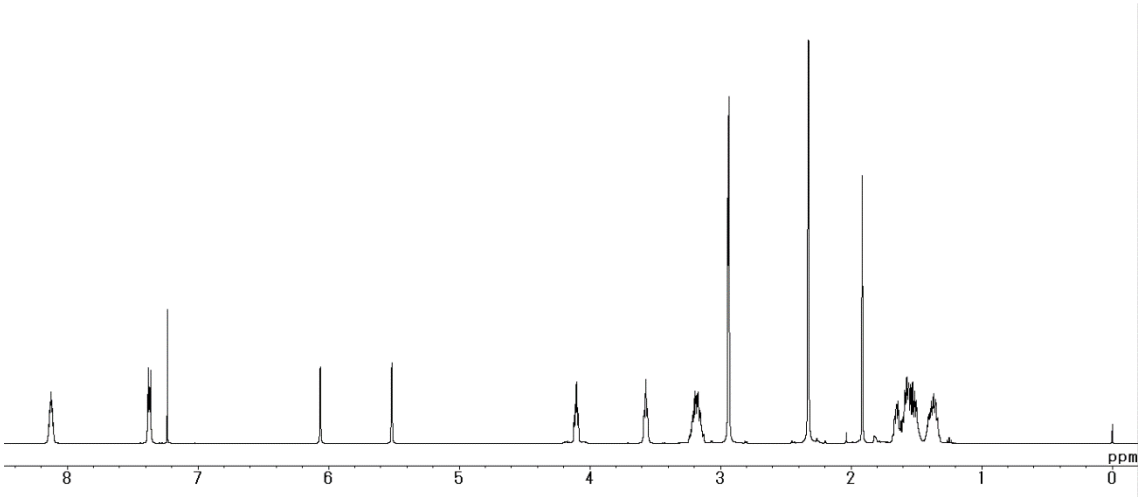

Fig. S19. ^{1}H NMR spectrum of methacrylate-monofunctionalized 1,4-bis(*N*-(hydroxypent-5-yl)-*N*-methylamino)-2,3-dimethylnaphthalene (**NAPH-monomer**) (500 MHz, $CDCl_3$).

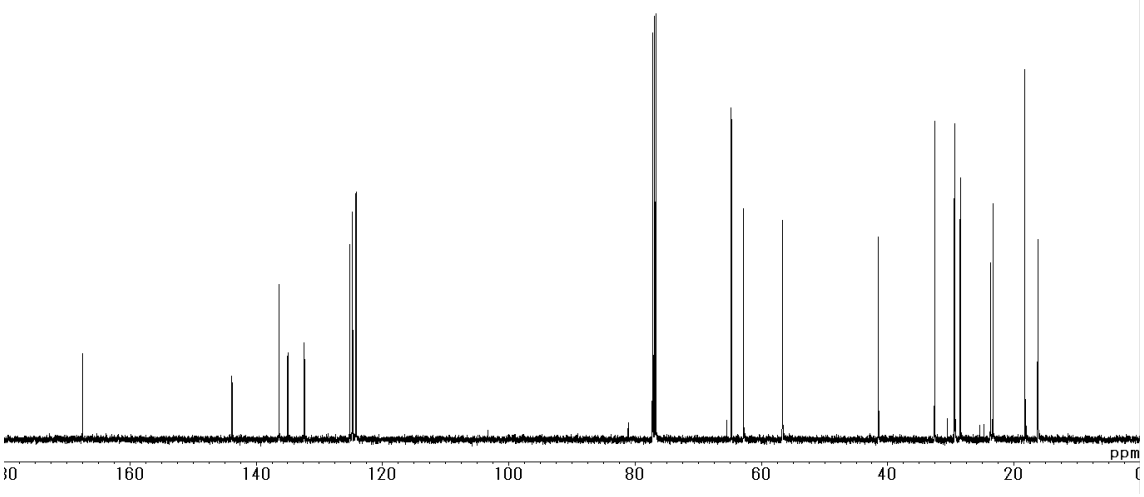

Fig. S20. ^{13}C NMR spectrum of methacrylate-monofunctionalized 1,4-bis(*N*-(hydroxypent-5-yl)-*N*-methylamino)-2,3-dimethylnaphthalene (**NAPH-monomer**) (125 MHz, $CDCl_3$).

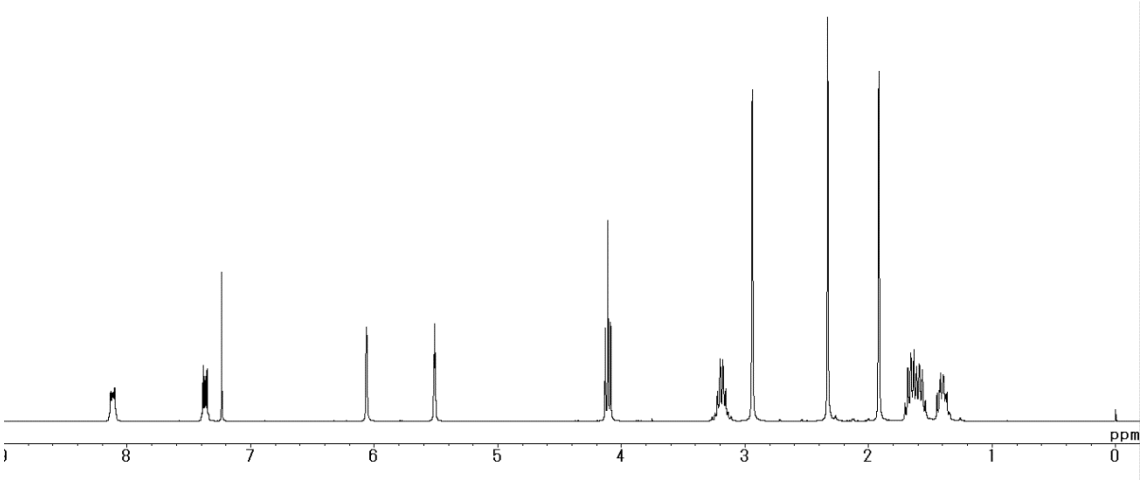

Fig. S21. ^{1}H NMR spectrum of methacrylate-difunctionalized 1,4-bis(*N*-(hydroxypent-5-yl)-*N*-methylamino)-2,3-dimethylnaphthalene (**NAPH-linker**) (300 MHz, $CDCl_3$).

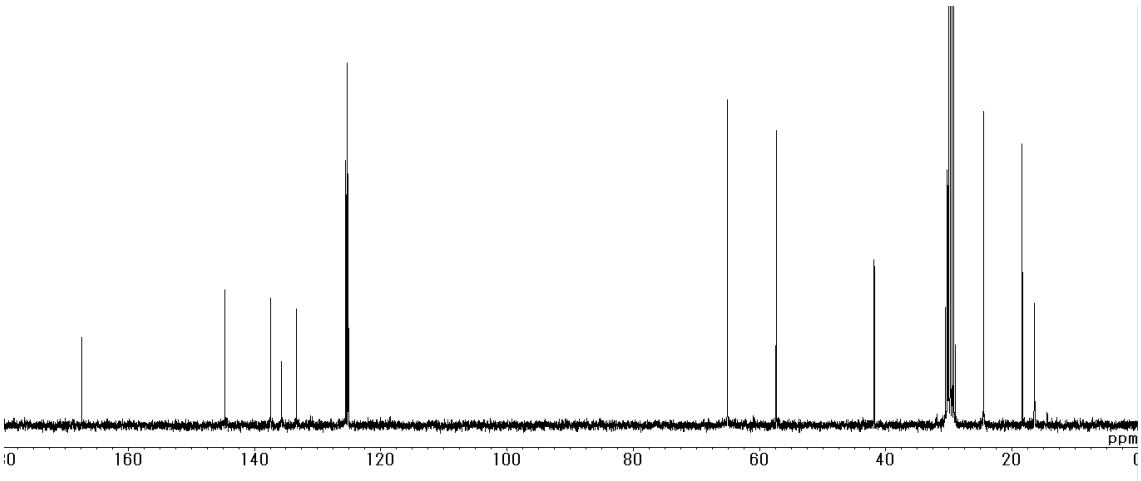

Fig. S22. ^{13}C NMR spectrum of methacrylate-difunctionalized 1,4-bis(*N*-(hydroxypent-5-yl)-*N*-methylamino)-2,3-dimethylnaphthalene (**NAPH-linker**) (75 MHz, acetone-d_6).

(3) Copolymer with *N*-isopropyl acrylamide (NIPAM)

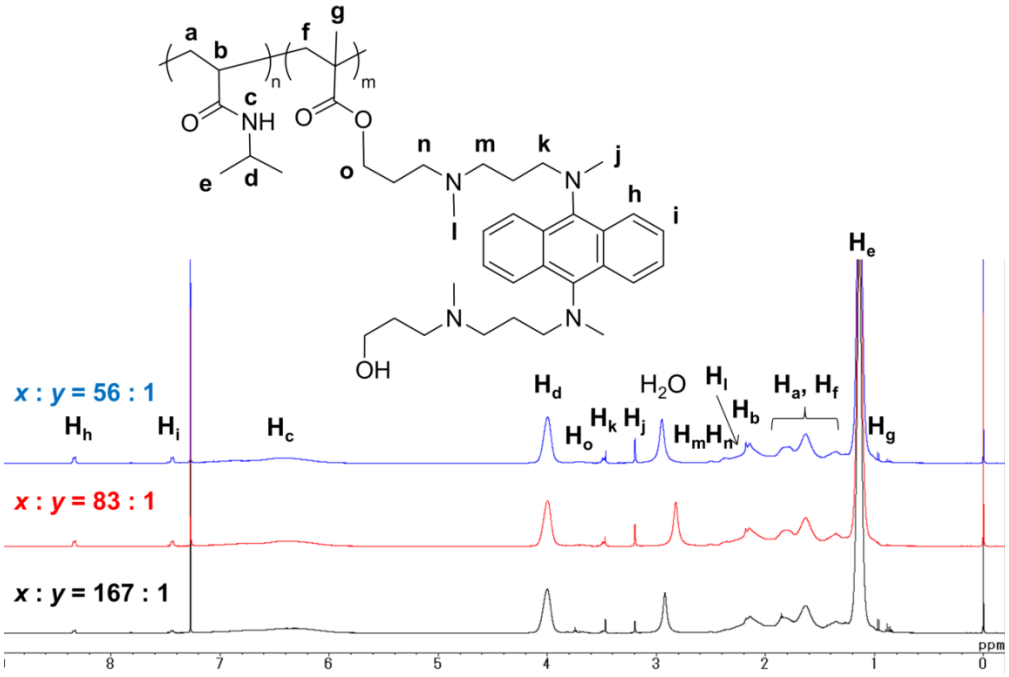

Fig. S23. ^{1}H NMR spectra of [**ANTH-polymer**]$_x$ prepared from different monomer feed ratios *x*:*y* (500 MHz, $CDCl_3$). The signal of water around 2.9 ppm is typically found in ^{1}H NMR spectra of PNIPAM derivatives measured in $CDCl_3$.[1]

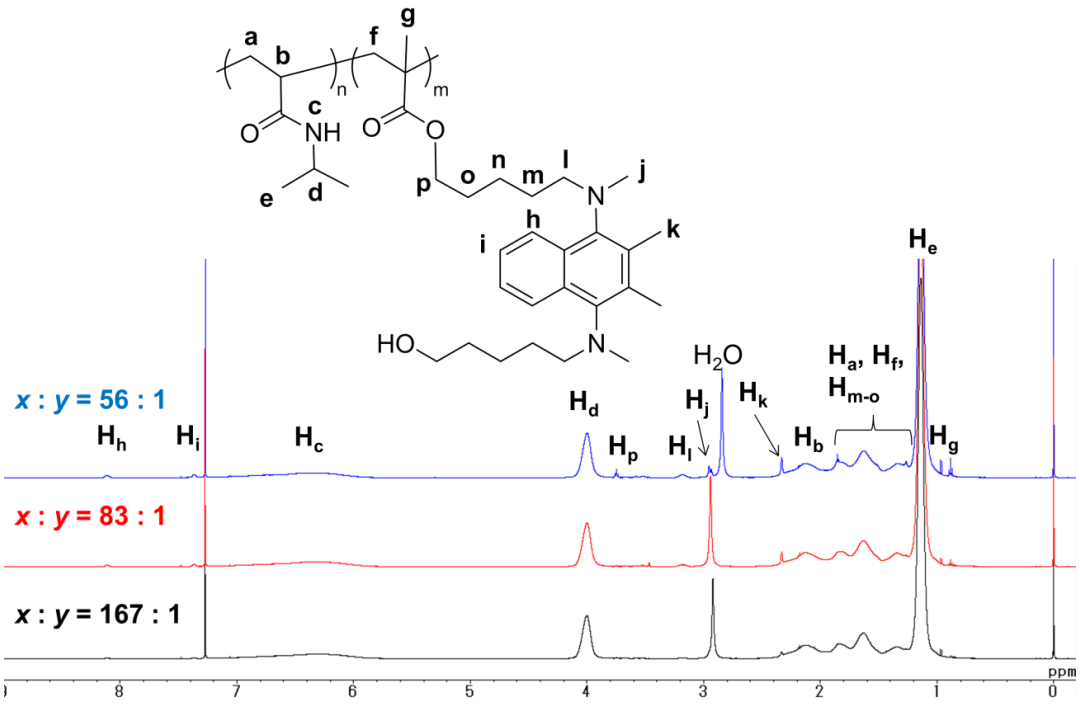

Fig. S24. ^{1}H NMR spectra of [**NAPH-polymer**]$_x$ prepared from different monomer feed ratios *x*:*y* (500 MHz, $CDCl_3$). The signal of water around 2.9 ppm is typically found in ^{1}H NMR spectra of PNIPAM derivatives measured in $CDCl_3$.[1]

S4. Size-exclusion chromatograms

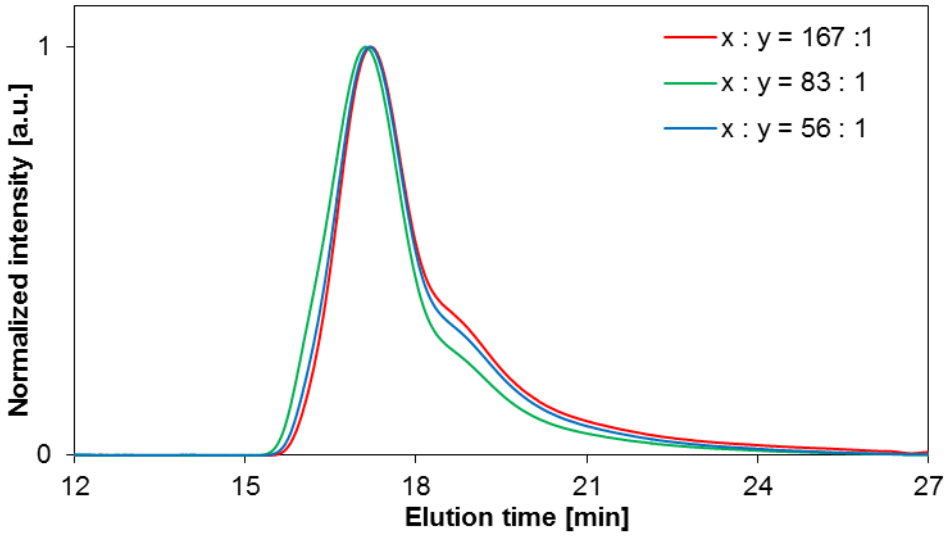

Fig. 25. SEC chromatograms for copolymer [**ANTH-polymer**]$_x$ prepared from different monomer feed ratios *x*:*y*.

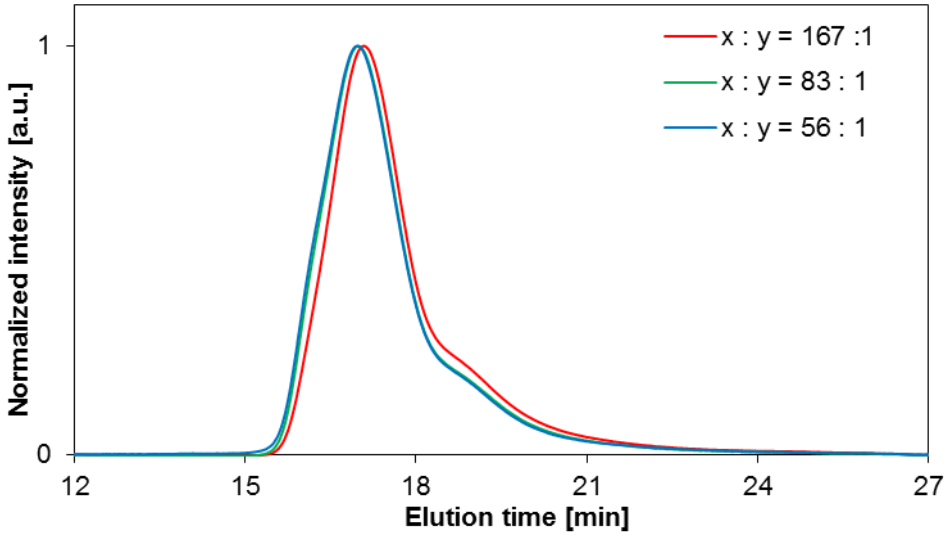

Fig. 26. SEC chromatograms for copolymer [**NAPH-polymer**]$_x$ prepared from different monomer feed ratios *x*:*y*.

S5. Photophysical properties

(1) Absorption and fluorescence spectra of monomers and crosslinkers

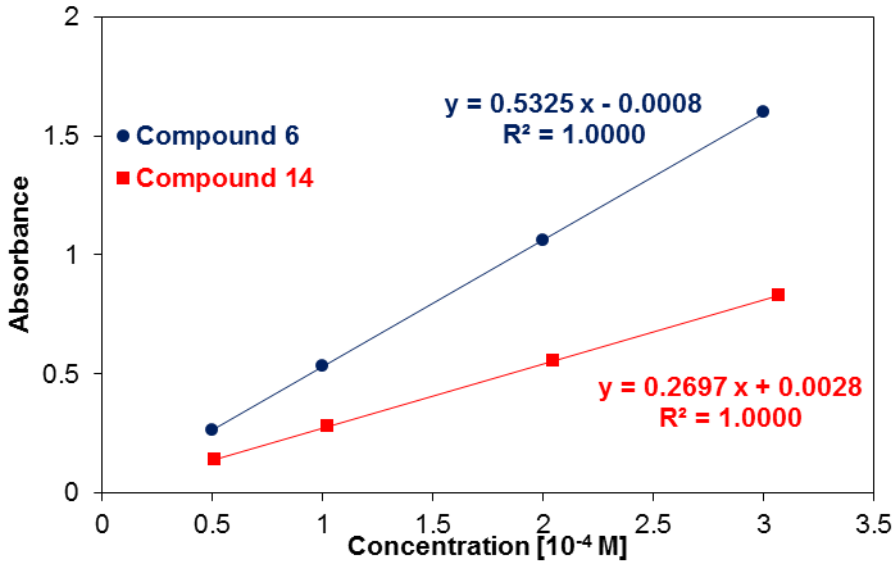

Fig. S27. Absorbance of **6** (at 401 nm) and **14** (at 321 nm) plotted as a function of the solute concentration. The calibration line was used to determine the concentration of each fluorophore in polymer solutions.

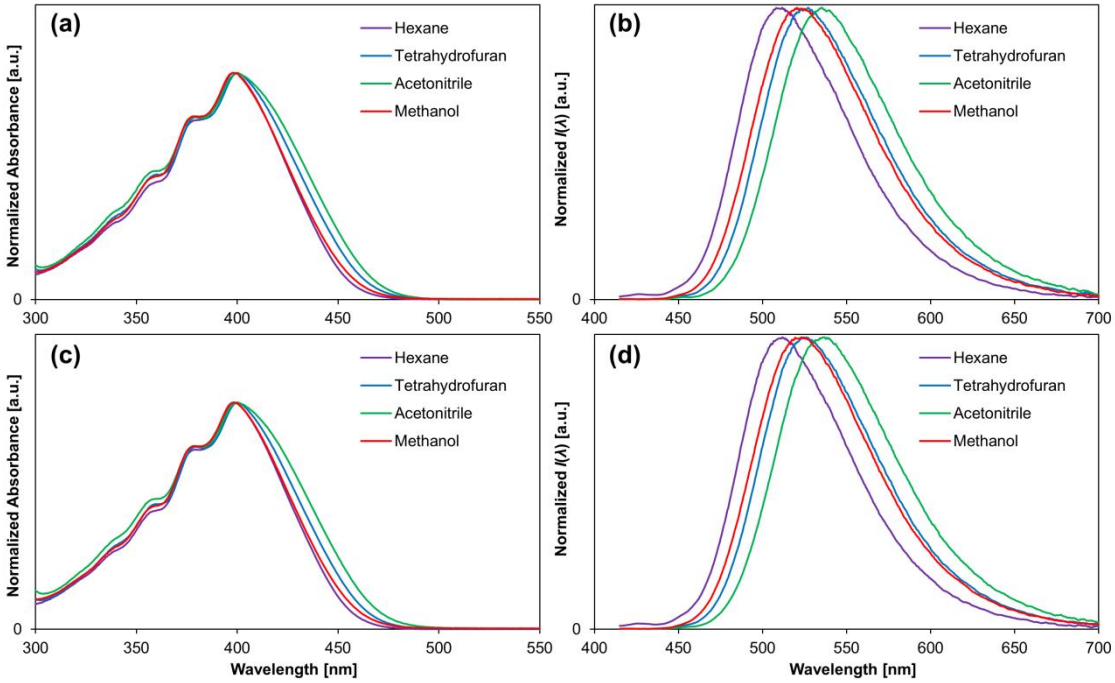

Fig. S28. (a) Absorption and (b) fluorescence spectra of **ANTH-monomer**; (c) absorption and (d) fluorescence spectra of **ANTH-linker**.

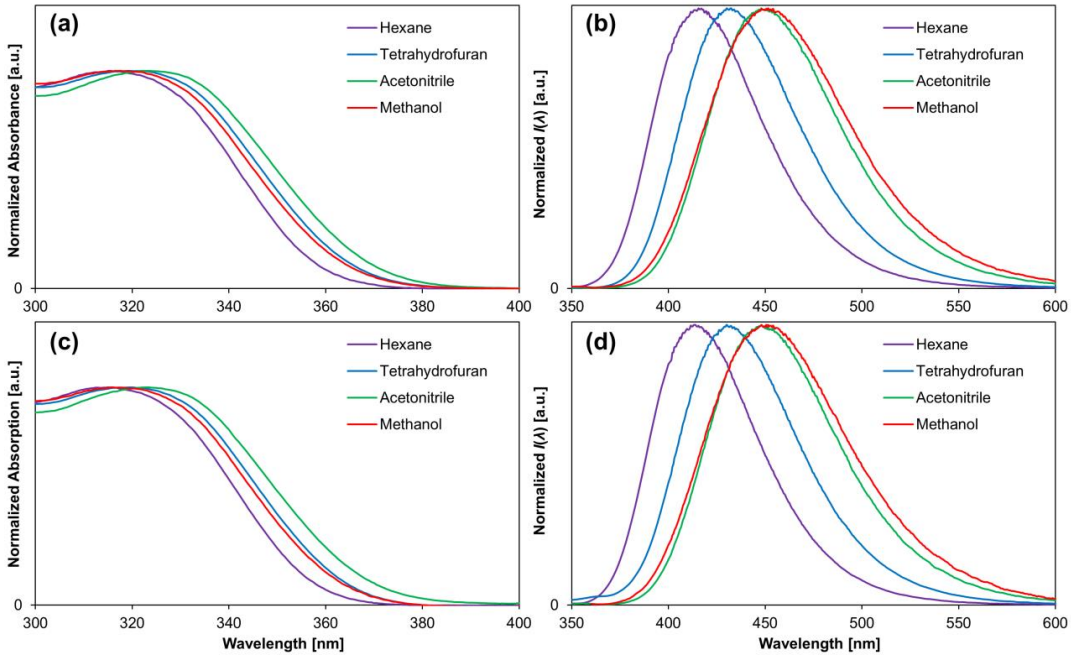

Fig. S29. (a) Absorption and (b) fluorescence spectra of **NAPH-monomer**; (c) absorption and (d) fluorescence spectra of **NAPH-linker**.

Table S1. Photophysical parameters of **ANTH-monomer**, **ANTH-linker**, **NAPH-monomer** and **NAPH-linker** measured in various solvents.

Entry	Solvent	λ_{abs} [nm]	λ_{fl} [nm]	Φ_{fl}	τ_{fl} [ns]	k_r [10^7 s^{-1}][a]	k_{nr} [10^7 s^{-1}][a]
ANTH-monomer	*n*-hexane	398	512	0.04	-	-	-
	Tetrahydrofuran	400	527	0.05	-	-	-
	Acetonitrile	400	535	0.03	-	-	-
	Methanol	398	521	0.03	-	-	-
ANTH-linker	*n*-hexane	399	512	0.04	-	-	-
	Tetrahydrofuran	400	526	0.05	-	-	-
	Acetonitrile	400	536	0.03	-	-	-
	Methanol	399	524	0.03	-	-	-
NAPH-monomer	*n*-hexane	316	416	0.09	-	-	-
	Tetrahydrofuran	320	432	0.20	2.94	6.7	27.3
	Acetonitrile	323	448	0.09	-	-	-
	Methanol	318	452	0.08	-	-	-
NAPH-linker	*n*-hexane	315	414	0.11	1.52	6.8	59.2
	Tetrahydrofuran	318	430	0.14	2.33	6.1	36.9
	Acetonitrile	323	448	0.04	-	-	-
	Methanol	317	451	0.03	-	-	-

[a] Rate constants were calculated based on the quantum yield measured with excitation wavelength λ_{ex} = 343 nm. The quantum yields measured with λ_{ex} = 343 nm are almost equal with that measured with λ_{ex} = fluorescence maxima.

(2) Absorption and fluorescence spectra of [ANTH-polymer]$_x$ and [NAPH-polymer]$_x$

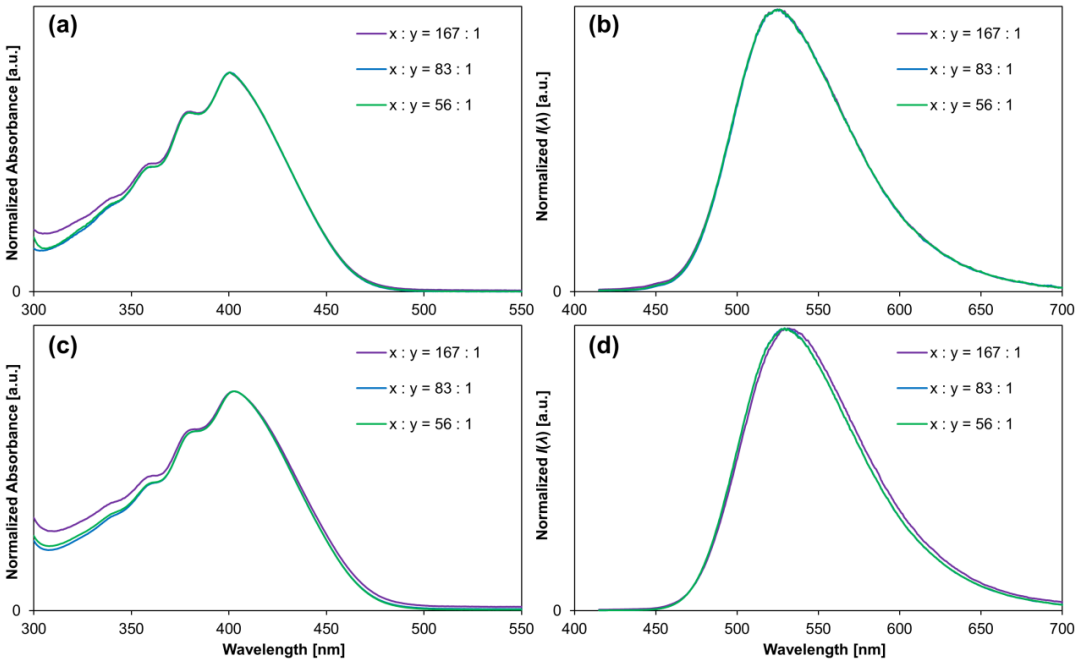

Fig. S30. (a),(c) Absorption and (b),(d) fluorescence spectra of [**ANTH-polymer**]$_x$ prepared using different monomer ratios *x*:*y*. (a) and (b) were obtained from THF solution, while (c) and (d) were obtained from water.

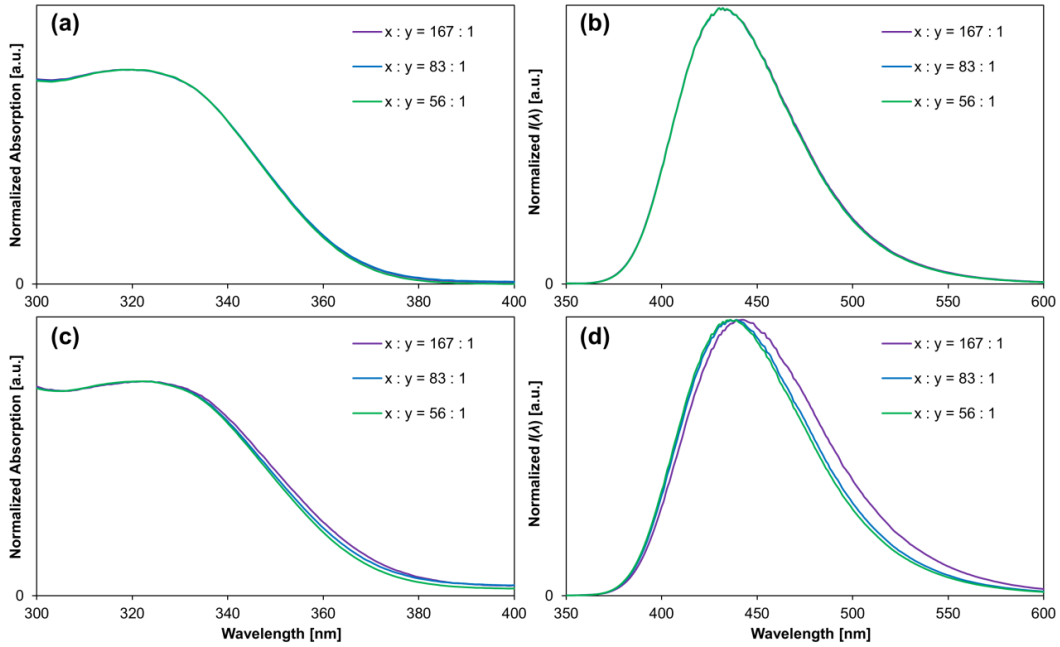

Fig. S31. (a),(c) Absorption and (b),(d) fluorescence spectra of [**NAPH-polymer**]$_x$ prepared using different monomer ratios *x*:*y*; (a) and (b) were obtained from THF solution, while (c) and (d) were obtained from water.

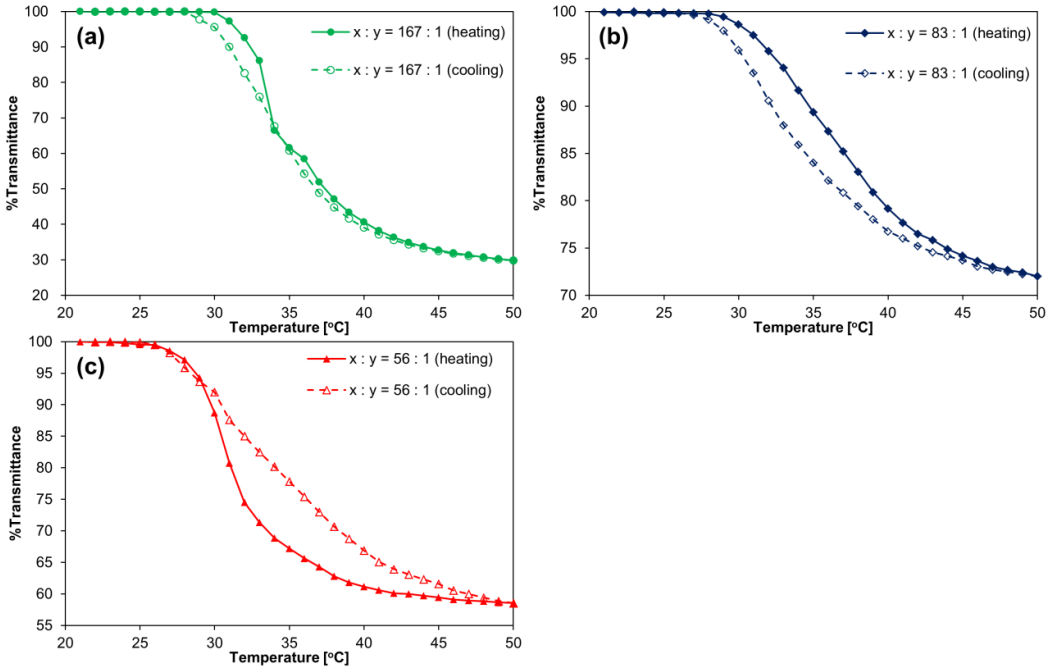

Fig. S32. Temperature dependence of the transmittance of (a) **[ANTH-polymer]**$_{167}$; (b) **[ANTH-polymer]**$_{83}$; and (c) **[ANTH-polymer]**$_{56}$ in H_2O. The transmittance was monitored at 650 nm (c_{solute} = 1 mg mL^{-1}).

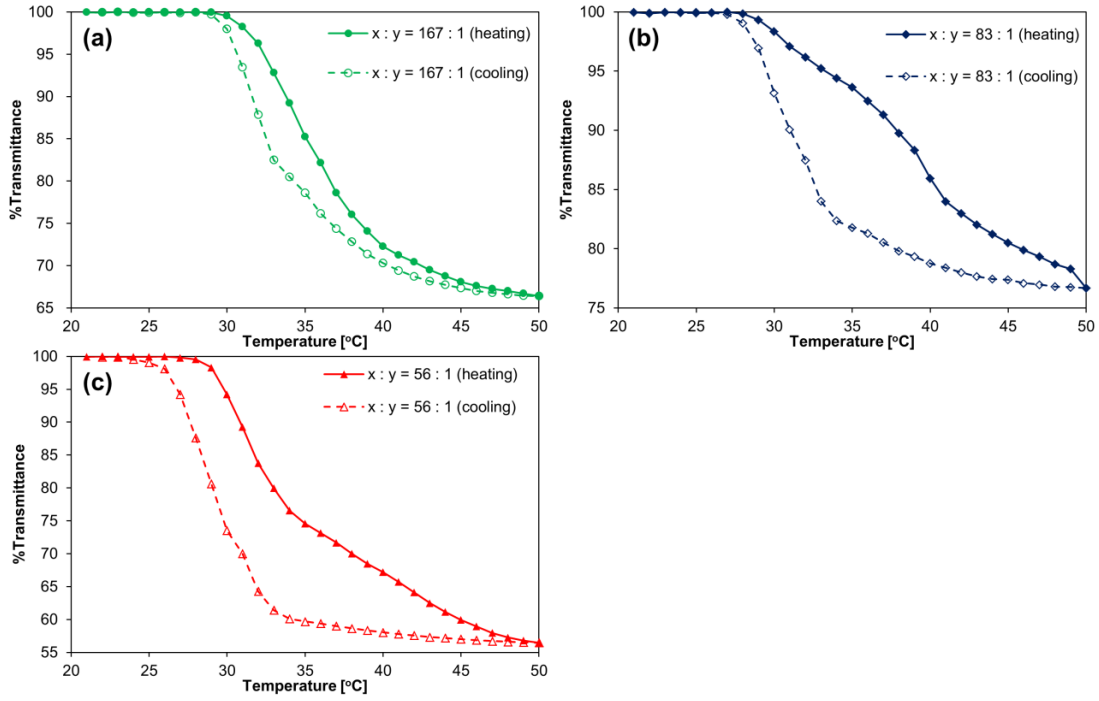

Fig. S33. Temperature dependence of the transmittance of (a) **[NAPH-polymer]**$_{167}$; (b) **[NAPH-polymer]**$_{83}$; and (c) **[NAPH-polymer]**$_{56}$ in H_2O. The transmittance was monitored at 650 nm (c_{solute} = 1 mg mL^{-1}).

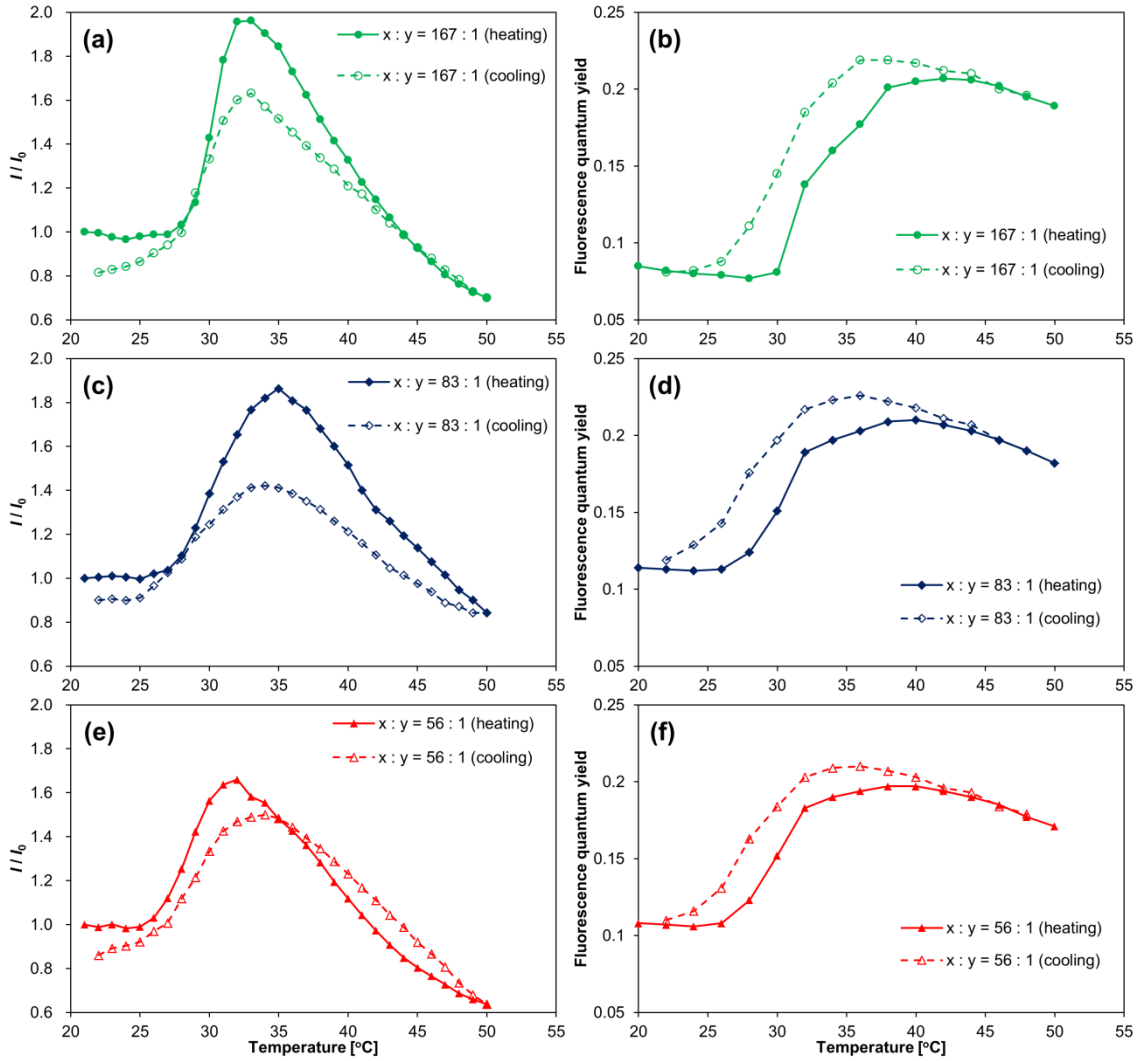

Fig. S34. Temperature dependence of the fluorescence intensity (I) and fluorescence quantum yields (Φ_{fl}) of (a), (b) **[ANTH-polymer]$_{167}$**; (c), (d) **[ANTH-polymer]$_{83}$**; and (e), (f) **[ANTH-polymer]$_{56}$** (I_0 = fluorescence intensity at ~ 530 nm; T = 21 °C, λ_{ex} = 403 nm, and c_{solute} = 1 g L^{-1}).

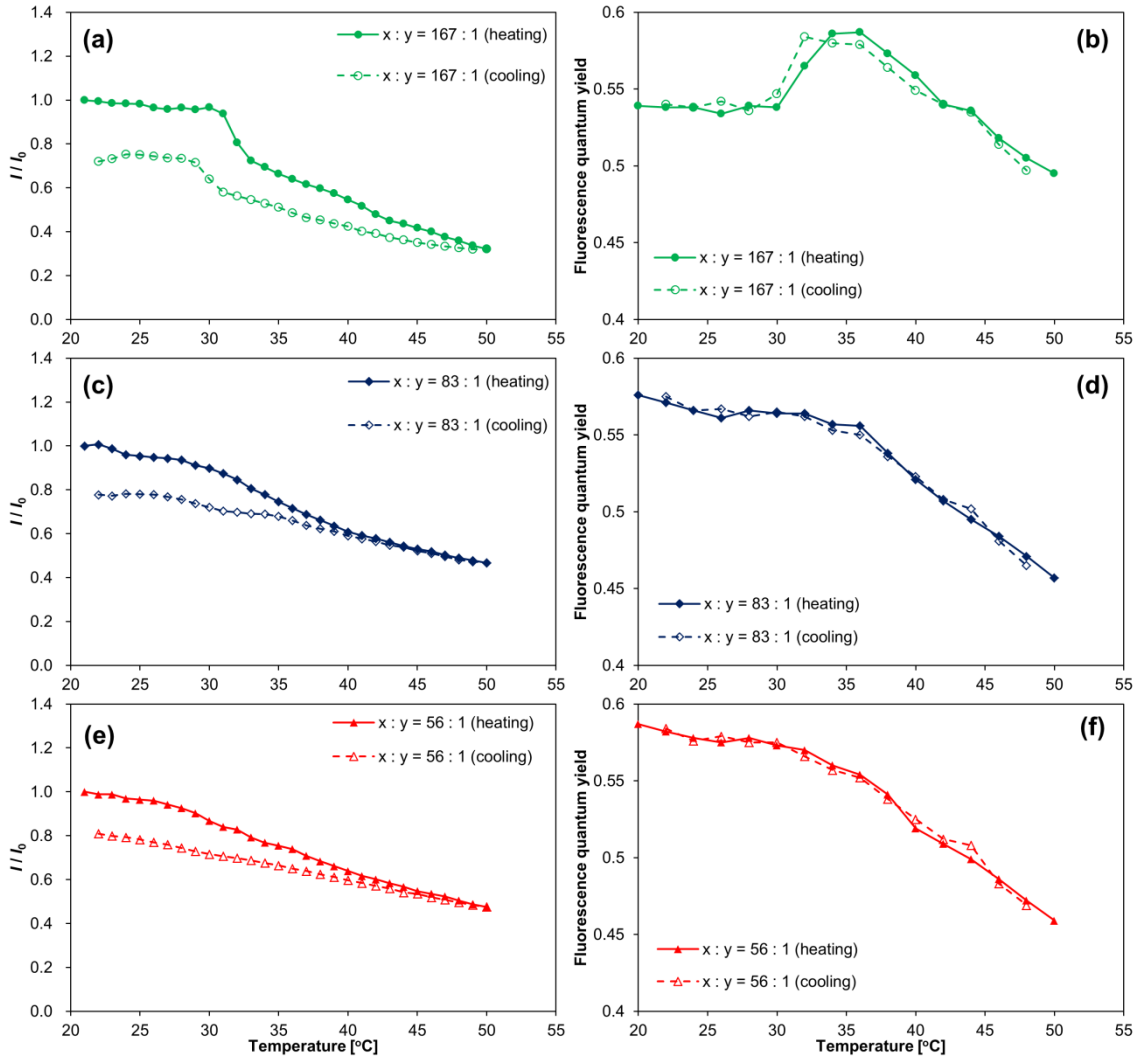

Fig. S35. Temperature dependence of the fluorescence intensity (I) and fluorescence quantum yields (Φ_{fl}) of (a), (b) **[NAPH-polymer]$_{167}$**; (c), (d) **[NAPH-polymer]$_{83}$**; (e), (f) **[NAPH-polymer]$_{56}$** (I_0 = fluorescence intensity at ~ 440 nm; T = 21 °C, λ_{ex} = 323 nm, and c_{solute} = 1 g L^{-1}).

S5. References

1. (*a*) A. Narumi, K. Fuchise, R. Kakuchi, A. Toda, T. Satoh, K. Kawaguchi, K. Sugiyama, A. Hirao and T. Kakuchi, *Macromol. Rapid Commun.*, 2008, **29**, 1126-1133; (*b*) M.; Iijima and Y. Nagasaki, *J. Polym. Sci. Part A: Polym. Chem.,* 2006, **44**, 1457-1469; (*c*) S.-W. Kuo, J.-L. Hong, Y.-C. Huang, J.-K. Chen, S.-K. Fan, F.-H. Ko, C.-W. Chu and F.-C. Chanf, *J. Nanomater.,* 2012, 749732.